Journal of Hydrology 542 (2016) 463–473

Contents lists available at ScienceDirect

Journal of Hydrology

journal homepage: www.elsevier.com/locate/jhydrol

Research papers

Non-linear hydraulic properties of woodchips necessary to design denitrification beds

Ehsan Ghane [a,*], Gary W. Feyereisen [b], Carl J. Rosen [a]

[a] Department of Soil, Water and Climate, University of Minnesota, Saint Paul, MN 55108, USA
[b] USDA Agricultural Research Service, Soil and Water Management Research Unit, Saint Paul, MN 55108, USA

ARTICLE INFO

Article history:
Received 30 January 2016
Received in revised form 16 July 2016
Accepted 7 September 2016
Available online 13 September 2016
This manuscript was handled by L. Charlet, Editor-in-Chief, with the assistance of Antonio Lo Porto, Associate Editor

Keywords:
Denitrifying bioreactor
Hydraulic conductivity
Hydraulic retention time
Temperature
Tile drainage
Woodchip bioreactor

ABSTRACT

Denitrification beds are being used to reduce the transport of water-soluble nitrate via subsurface drainage systems to surface water. Only recently has the non-linearity of water flow through woodchips been ascertained. To successfully design and model denitrification beds with optimum nitrate removal, a better understanding of flow in denitrification beds is needed. The main objectives of this study were to characterize the hydraulic properties of old degraded woodchips and provide a better understanding of the factors affecting flow. To achieve this goal, we conducted constant-head column experiments using old woodchips that were excavated from a four-year old denitrification bed near Willmar, Minnesota, USA. For Izbash's equation, the non-Darcy exponent (n) ranged from 0.76 to 0.87 that indicates post-linear regime, and the permeability coefficient (M_{10}) at 10°C ranged from 0.9 to 2.6 cm s^{-1}. For Forchheimer's equation, the intrinsic permeability of 5.6×10^{-5} cm^2 and ω constant of 0.40 (at drainable porosity of 0.41) closely resembled the in-situ properties found in a previous study. Forchheimer's equation was better than that of Izbash's for describing water flow through old woodchips, and the coefficients of the former provided stronger correlations with drainable porosity. The strong correlation between intrinsic permeability and drainable porosity showed that woodchip compaction is an important factor affecting water flow through woodchips. Furthermore, we demonstrated the importance of temperature effects on woodchip hydraulics. In conclusion, the hydraulic properties of old woodchips should be characterized using a non-Darcy equation to help design efficient systems with optimum nitrate removal.

© 2016 Elsevier B.V. All rights reserved.

1. Introduction

Agricultural subsurface drainage facilitates the removal of excess water from the soil profile to provide soil aeration, timely field operations, and reduce surface erosion. While subsurface drainage helps improve crop production, it can also transport some nitrate to surface water from organic matter mineralization as well as from nitrogen fertilizers used to produce crops. Elevated concentrations of nitrate in surface water can contribute to hypoxia and toxin production from harmful algal blooms (USEPA, 2013; Horst et al., 2014; Harke and Gobler, 2015). Denitrifying bioreactors are one approach for removing nitrate from water by providing a carbon source for the biological transformation (i.e., denitrification) of nitrate into di-nitrogen gas. One type of a denitrifying bioreactor is a denitrification bed (also known as a woodchip bioreactor) that can reduce nitrate concentration from subsurface drainage water (Schipper et al., 2010; Bednarek et al., 2014). In denitrification beds (hereafter referred to as bed), woodchips have been commonly used as the carbon medium.

Accurate characterization of hydraulic properties of woodchips is vital for the successful design and modeling of beds to achieve optimum nitrate removal. The design guideline of beds in the Midwest USA has been developed based on the hydraulic properties of woodchips assuming Darcian flow (USDA NRCS, 2015). However, Ghane et al. (2014) showed overestimation of the peak flow rate of a bed using Darcy's law under field conditions, which in turn, results in underestimation of the actual hydraulic retention time at the peak flow rate of the bed. As a result, bed designs can be overly long and have undersized width according to the non-Darcy flow component of the bed model in Ghane et al. (2015). Beds that are too long increase the potential for undesirable consequences when nitrate concentration is depleted within the bed, i.e., reduction of sulfate to hydrogen sulfide and inorganic mercury to methylmercury (Shih et al., 2011). Therefore, there is a need for characterizing water flow through woodchips using the governing

* Corresponding author.
E-mail addresses: ehsan.ghane@outlook.com, eghane@umn.edu (E. Ghane).

http://dx.doi.org/10.1016/j.jhydrol.2016.09.021
0022-1694/© 2016 Elsevier B.V. All rights reserved.

flow equation in laboratory column experiments, so the results can be used to adjust bed design guidelines, and in turn, provide systems that are more efficient.

For many years, water flow through woodchips was assumed to follow Darcy's law in laboratory experiments without validation of linear flow (Chun et al., 2009; Cameron and Schipper, 2010; Leverenz et al., 2010; Schmidt and Clark, 2013; Krause Camilo et al., 2013; Subroy et al., 2014; Goodwin et al., 2015). These studies reported a range of woodchip hydraulic conductivities from 0.01 to 54 cm s^{-1}. Leverenz et al. (2010) calculated one of the highest woodchip hydraulic conductivities ever reported (i.e., 54 cm s^{-1}). However, the related work by Hopes (2010) presents evidence that suggests their reported value is too high.

Darcy's law has also been used to provide a rough estimate of hydraulic conductivity in the field based on assumptions and without validation of linear flow (Van Driel et al., 2006; Robertson et al., 2009; Robertson and Merkley, 2009). In one of these studies, Robertson et al. (2009) found a wide range of hydraulic conductivities from 0.3 to 5 cm s^{-1} for a bed assuming 90% of the water flows through the coarse woodchips for the first two years and 100% from year two to seven. David et al. (2016) attempted to determine the in-situ hydraulic conductivity of woodchips in a bed, but they encountered a non-linear relationship between specific discharge and hydraulic gradient that did not allow them to determine a definite in-situ hydraulic conductivity based on Darcy's law. More recently, Krause Camilo (2016) reported a hydraulic conductivity of 10 cm s^{-1} for a mixture of bark mulch chips and straw in a pilot-scale bed based on Darcy's law and without validation of linear flow.

Only recently has the non-linearity of water flow for fresh (Feyereisen and Christianson, 2015) and old woodchips (Ghane et al., 2014) been ascertained in laboratory column experiments. Thus, reports of woodchip hydraulic properties using the governing non-linear flow equation are scarce. Therefore, a need exists to determine the hydraulic properties of woodchips for non-Darcy flow in laboratory column experiments. In particular, old woodchip properties are of great importance because they represent the woodchips that have been under natural conditions in a bed, and they have been found to have different properties than fresh woodchips (Robertson, 2010; Ghane et al., 2014). While laboratory experiments have ascertained the non-linearity of water flow through woodchips, this has not been shown in a bed under field conditions. Therefore, there is a need for graphical evaluation of the non-linearity of water flow through a bed in a field experiment.

Drainable porosity (specific yield) is an important property of woodchips, which can be used instead of effective porosity to calculate the actual hydraulic retention time (*HRT*) when the latter is unavailable from tracer testing. However, there are only a few laboratory column studies that have calculated the drainable porosity of old woodchips. Ghane et al. (2014) calculated drainable porosities of 0.37–0.39 for the two-year, two-month old woodchips, and Robertson (2010) calculated a value of 0.46 for seven-year old woodchips when draining the water for 1 h. Some studies have assumed much higher values (i.e., 0.70) for woodchip beds under field conditions (Bell et al., 2015; Rambags et al., 2016). Therefore, there is a need for more experiments to obtain better estimates of drainable porosity of old woodchips.

Temperature is another important parameter in woodchip hydraulics. Temperature effect on soil hydraulic properties is well known (Gao and Shao, 2015), but this effect for water flow through woodchip media has never been shown previously. Some studies have accounted for the effect of temperature on woodchip hydraulic conductivity (Ghane et al., 2014; Feyereisen and Christianson, 2015), and some studies have not (Van Driel et al., 2006; Chun et al., 2009; Robertson et al., 2009; Robertson and Merkley, 2009; Cameron and Schipper, 2010; Schmidt and Clark, 2013; David et al., 2016). Those that did not account for this effect could have had temperature as a confounding variable affecting specific discharge, and thereby, affecting hydraulic conductivity. Therefore, there is a need to evaluate the effect of temperature on hydraulic properties of woodchips.

Although hydraulic properties of old woodchips are essential to the design and modeling of beds, we found only one study that had reported those values while validating the Darcian flow. In that study, Ghane et al. (2014) reported the first laboratory and in-situ hydraulic properties of old woodchips using Forchheimer's equation. A review of the literature shows that there is a need to better understand the non-Darcian flow, and determine the hydraulic properties of old woodchips using other flow equations such as Izbash's law, for which, to our knowledge, has never been investigated for woodchips in its entirety.

The objectives of this study were to (1) graphically evaluate Darcy's law for water flow through old woodchips in a permeameter and in a bed under field conditions, (2) determine the hydraulic properties (i.e., flow coefficients and drainable porosity) of old woodchips, (3) compare the performance of Forchheimer's equation to that of Izbash's in describing the flow, (4) determine the error of ignoring the non-Darcy flow, and (5) evaluate the effect of temperature on hydraulic properties. The practical importance of this study is that it provides essential information that is required to design efficient denitrification beds in which undesirable consequences are minimized.

2. Theory

2.1. Pre-linear, linear, and post-linear flow

The theory of water flow through porous media is fundamental to a wide range of disciplines. Basak (1977b) identified three main zones for water flow through porous media for a range of hydraulic gradients (Fig. 1). These zones are pre-linear, linear and post-linear zones. The former occurs when water flows through porous media at very low velocities. For this zone, specific discharge (apparent velocity) is not proportional to hydraulic gradient. For the linear zone, water velocity is low, so specific discharge is proportional to hydraulic gradient. In this zone, soil scientists commonly apply Darcy's (1856) law for water flow through soils.

For the post-linear zone, the linear relationship between specific discharge and hydraulic gradient does not exist due to the high water velocities in the porous media (Basak, 1977a). In this zone, the increase in specific discharge is proportionally smaller than the increase in hydraulic gradient. This is because inertial forces

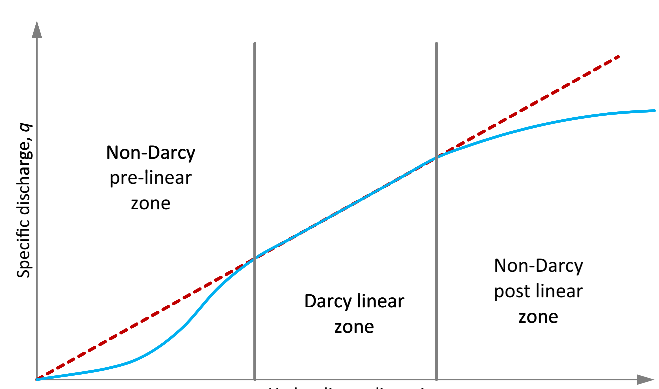

Fig. 1. Diagram of the three main zones for water flow through porous media. The dotted line represents Darcian flow (modified from Basak, 1977b).

become substantial compared to viscous forces at high water velocities (Bear, 1988). Examples of post-linear regimes are water flow through sand (Soni et al., 1978), gravel (Sadeghi-Asl et al., 2014), rock fractures (Chen et al., 2015), geosynthetic materials (Bordier and Zimmer, 2000), highway pavement (Dan et al., 2016), and confined aquifers (Wen et al., 2013; Wang et al., 2015).

2.2. Intrinsic permeability

According to Hubert (1940) hydraulic conductivity can be calculated from intrinsic permeability as

$$k = \frac{k_{in}\rho g}{\mu} \tag{1}$$

where k is hydraulic conductivity (cm s^{-1}), k_{in} is intrinsic permeability (cm^2), ρ is water density (g cm^{-3}), g is gravity acceleration (cm s^{-2}), and μ is water dynamic viscosity (g cm^{-1} s^{-1}). The benefit of using intrinsic permeability is that it is the property of the porous medium (e.g., woodchips), and it is independent of fluid properties (e.g., temperature).

2.3. Forchheimer's equation

Forchheimer's (1901) equation is commonly used to describe linear and post-linear flow regimes, and is written as

$$-i = \frac{1}{k_F} q + \omega q^2 \tag{2}$$

where q is specific discharge (cm s^{-1}), k_F is Forchheimer's hydraulic conductivity (cm s^{-1}), ω is a constant (s^2 cm^{-2}) that incorporates the non-Darcy coefficient or inertial coefficient, and i is hydraulic gradient (cm cm^{-1}) that is the ratio of head loss (ΔH) to length over which head loss has occurred (L). In the linear flow regime ($\omega = 0$), Forchheimer's equation shrinks to Darcy's equation ($k_F = k_D$ and $q = -k_D i$). The two unknown coefficients (k_F and ω) are determined by fitting a quadratic equation (with zero intercept) to the plot of the hydraulic gradient versus specific discharge. Then, Eq. (1) can be used to determine the intrinsic permeability.

2.4. Izbash's equation

Izbash's (1931) equation is an empirical equation that can be used to describe all three zones of pre-linear, linear and post-linear flow regimes, and is written as

$$q = -Mi^n \tag{3}$$

where M is the permeability coefficient (cm s^{-1}), and n is the non-Darcy exponent that is $0.5 < n < 1$ for post-linear regime. In the linear flow regime ($n = 1$), Izbash's equation reduces to Darcy's equation ($M = k_D$). The two unknown coefficients (M and n) are determined by fitting a linear equation to the plot of the log specific discharge versus log hydraulic gradient ($M = 10^{intercept}$ and $n = slope$).

Some studies have used Izbash's equation to describe water flow in confined aquifers (Wen et al., 2013; Wang et al., 2015). For describing the water flow through woodchips, Feyereisen and Christianson (2015) used a power function of the same structure as Izbash's equation. In that study, the authors determined the hydraulic conductivity of fresh woodchips by plotting the natural log q versus natural log i and finding the intercept of the linear regression. However, the authors did not report nor discuss the slope of the regression line, which is the non-Darcy exponent (n) that describes the flow. Therefore, to our knowledge, our study is the first to use the Izbash equation in its entirety to describe water flow through woodchip media.

2.5. Forchheimer number and non-Darcy effect

We used Forchheimer number (Fo) as an indicator of non-Darcy flow for water flow through woodchips (Zeng and Grigg, 2006), which is written as

$$Fo = \frac{\omega k_{in}\rho g q}{\mu} \tag{4}$$

We also used the non-Darcy error (E) to indicate the error of ignoring the non-Darcy effect. The non-Darcy effect increases with the increase in specific discharge (Zeng and Grigg, 2006), and is written as

$$E = \frac{Fo}{1 + Fo} \tag{5}$$

3. Materials and methods

3.1. Old woodchip acquisition

We collected woodchips from a plastic-lined bed (106.4 m long and 1.7 m wide) installed in November 2010 on a private farm near Willmar, Minnesota, USA (Supplementary Image 1). We excavated the bed using a backhoe (Supplementary Video 1), and took 20-L samples from the entire depth at approximately equal lengths along the bed (i.e., 0, 12.5, 25.9, 39.3, 52.7, 66.1, 79.6, 93.0, and 106.4 m) in October 2014. Samples were kept in a cooler until particle size analysis (Section 3.2). Furthermore, additional woodchip media along the bed length were collected and combined to yield a composite sample (i.e., representing the entire length) (Supplementary Image 2). These composite old woodchips were transported to the Engineering and Fisheries Laboratory, University of Minnesota, where their hydraulic properties were determined from April to November 2015. The three-year, eleven-month old woodchips were comprised of a mixed species of wood.

3.2. Particle size analysis

ASTM standard sieves were used to conduct a particle size analysis of the old woodchips (i.e., sampled along the bed length). After the woodchips were oven dried at 40°C for 24 h, they were allowed to equilibrate with room temperature for 24 h. This was done to avoid a change in woodchip mass during shaking due to absorbing humidity. After equilibrating, they were shaken for 15 min in a sieve shaker (Meinzer II) with screen sizes 25, 19, 12.5, 9.5, 8.0, 6.3, 4.75, 3.35, 1.18 mm. We performed five replicates for each sample, and used the particle size distribution to determine the d_{50} (i.e., diameter at which 50% of particles are finer) of the old woodchips. The average d_{50} along the length of the bed was used to calculate the Reynolds number (Fetter, 2001).

3.3. Permeability experiments

3.3.1. Permeameter

We used the constant head permeameter from Feyereisen and Christianson (2015) with minor adjustments (Fig. 2). Briefly, we used a PVC pipe (250 cm length and 30.3 cm inside diameter) with upward flow to minimize preferential flow (Supplementary Video 2). Different flow rates were established by adjusting the globe valve. Flow rate was measured using a bucket and stopwatch. The column had two caps at each end with springs pushing on steel screens to hold the woodchips in place (Supplementary Images 3 and 4). A submersible utility pump (Model 2VAN7, Dayton Electronics Manufacturing Co., Niles, Illinois, USA) was used to pump the municipal water source to the constant head structure.

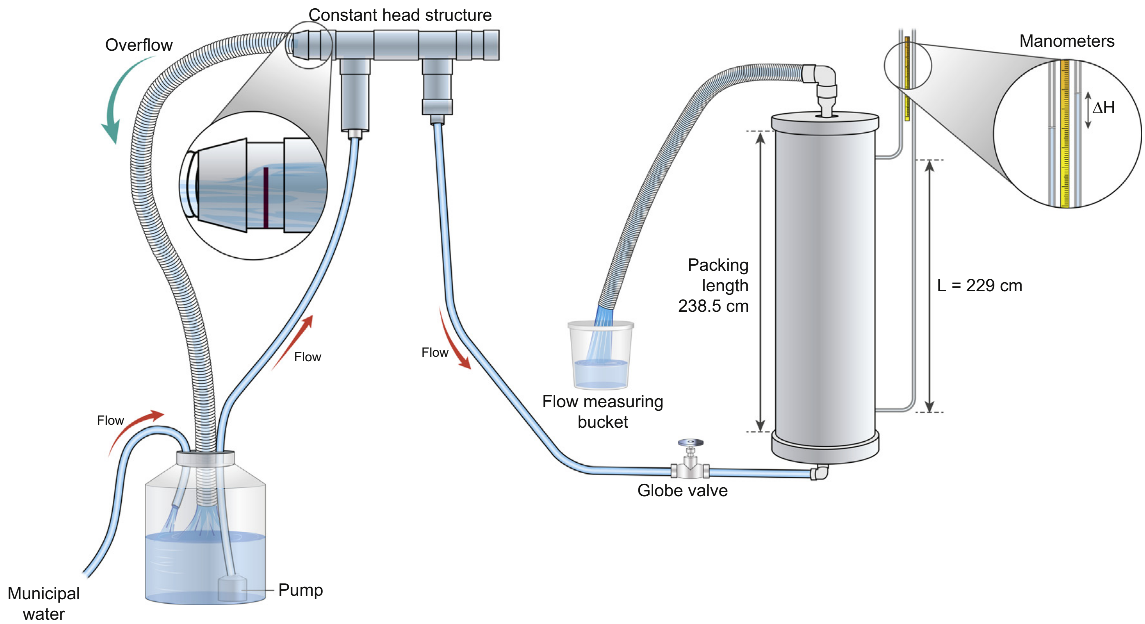

Fig. 2. Diagram of the permeameter (30.3 cm inside diameter) used to determine the hydraulic properties of old woodchips.

3.3.2. Woodchip compaction

We weighed and poured woodchips inside the column in 10-L increments. After each increment, a wooden plate was lowered onto the surface of the woodchips, and a 5.6 kg tamper was dropped on top of the plate from a constant height (i.e., a value between 30 and 50 cm) until the column was packed to the desired height (Supplementary Image 5). The reason for using a plate was to distribute the impact force onto the woodchip surface uniformly. We also did not shake the column as in Feyereisen and Christianson (2015), believing that it better represents field conditions. We conducted seven independent experiments, each time packing a fresh batch of the composite old woodchips. Among the seven experiments, different drop heights of the tamper were used to get a range of drainable porosities.

In addition to the seven independent experiments, we conducted three dependent experiments (i.e., experiments U-1 to U-3) by packing a used batch of the composite old woodchips. In other words, after draining the column following the independent experiments, we emptied the column and placed the woodchips on a tarp to air dry. When these woodchips were visually similar to the woodchips of the independent experiments in terms of moisture, we used them to re-pack the column for three dependent experiments. Results from the independent experiments are discussed in Section 4.3.1.

3.3.3. Permeability measurement

After filling the column, we allowed the woodchips to sit saturated overnight before initiating the permeability experiment. The reason for the saturation was that woodchip particles would swell by absorbing water before the experiment rather than swelling during the experiment and thereby, modifying the permeability. Also, the woodchip saturation is more representative of field conditions. At the beginning of each experiment, municipal water flowed through the column until the outflow water temperature had stabilized. After this stabilization period, we recorded flow rate and head difference with every increase in the hydraulic gradient up to a maximum of 0.086. The hydraulic gradients generated in this experiment were anticipated to be within the naturally occurring range under field conditions in a bed.

Outflow water temperature was recorded continuously using a digital thermometer (4354 Traceable Long-Stem Thermometer, Friendswood, TX, USA). For each experiment, Forchheimer's and Izbash's coefficients, and R-square of their fits were determined using SAS 9.4 (SAS Institute Inc., Cary, NC). The R-square for Izbash's equation was based on the linear relationship between log specific discharge versus log hydraulic gradient.

3.4. Drainable porosity

Immediately after each permeability experiment (i.e., seven independent and three dependent experiments), we removed the top column cap and adjusted the water level to the top of the woodchips. The top cap was put loosely in place to prevent evaporation, and the column was allowed to drain for 24 h while measuring the water volume. The volume of the bottom cap (4215 cm^3) was subtracted from the total water volume drained to yield the adjusted drained water volume. Drainable porosity (specific yield) was calculated from dividing the adjusted drained water volume by the woodchip packing volume. Drainable porosity has sometimes been incorrectly referred to as primary porosity. We advise against using this term, since the latter is the original porosity formed under sediment deposition during the time of diagenesis (Bear, 1988; Fetter, 2001; Sen, 2015).

3.5. Graphical evaluation of non-Darcy flow in a denitrification bed

To evaluate non-linearity of water flow in a bed, we used the V-notch weir calibration data from Ghane et al. (2014) that was performed in a trapezoidal bed under field conditions in Ohio, USA. Briefly, calibration was conducted in one day with 14 flow rates ranging from 94 to 535 $cm^3\ s^{-1}$. The initial flow rate was allowed to run for 1 h and 30 min, and then decreased to 40 min for the subsequent flow rates, before the inflow and outflow water heights of the bed were recorded. This was conducted under minimal outflow temperature variations (i.e., 20.1 °C ± 0.6 °C, average ± SD); thus, the confounding effect of temperature was eliminated.

Unlike column experiments where the area of flow is constant, the area of flow varies along the length of a bed. Hence, specific discharge varies along the length of a bed, so we cannot use the typical relationship between q and i to evaluate the conformity of data to Darcy's law. To achieve this, we used the Darcian flow rate equation for a trapezoidal bed developed by Ghane et al. (2014), which is written as

$$Q = k_D \left[\frac{b\left(h_i^2 - h_o^2\right)}{2L_B} + \frac{z\left(h_i^3 - h_o^3\right)}{3L_B} \right] \quad (6)$$

where Q is flow rate of a trapezoidal bed (cm^3 s^{-1}), h_i and h_o are bed inflow and outflow heights of water (cm), L_B is length of bed (825 cm), b is bottom width of a bed (265 cm), k_D is Darcy's hydraulic conductivity (cm s^{-1}), and z is side slope of 0.5 (z:1, width: height). In the plot of Q versus the bracket component, the slope of the line should be k_D under laminar flow conditions.

4. Results and discussion

4.1. Particle size analysis

Particle size distribution of old woodchips provided the mean d_{50} values along the length of the bed. The average of the d_{50} values along the length of the bed was 9.1 ± 0.5 mm. Our d_{50} value was slightly larger than the average d_{50} of 7.6 ± 0.1 mm for a different source of a mixed species of old woodchips in Ohio (Ghane et al., 2014). It is important to note that the d_{50} values reported here mostly represent the length of the woodchip particles, since its length allowed the woodchips to be retained on each sieve.

4.2. Graphical confirmation of non-Darcy flow

4.2.1. Non-Darcy flow in a column

If Darcy's law applies to water flow through woodchips, the relationship between specific discharge and hydraulic gradient should be linear. Fig. 3 shows non-linear patterns consistent with post-linear regimes for old woodchips (see Interactive Plots for data). In our experiments, we did not find any linear feature at low hydraulic gradients. Therefore, the lowest hydraulic gradient is considered to be the point of departure from linearity. The non-linearity of water flow through fresh (Feyereisen and Christianson, 2015) and old woodchips (Ghane et al., 2014) has been reported previously.

4.2.2. Non-Darcy flow in a denitrification bed

The flow rate and bed water heights (i.e., inflow and outflow) from the V-notch weir calibration data of Ghane et al. (2014) were used in Eq. (6) to evaluate non-Darcy flow in a bed. Results showed that the plot of Q versus the bracket component of Eq. (6) did not result in a straight line that would have signified laminar flow conditions (Fig. 4) (see Interactive Plots for data). Therefore, Darcy's law could not explain water flow through a bed under field conditions. To our knowledge, this is the first graphical confirmation of non-Darcian flow in a bed.

Graphical confirmation of non-Darcian flow under field conditions is challenging, since water temperature during the experiment needs to stay relatively constant to avoid being a confounding variable. David et al. (2016) showed a non-linear relationship between specific discharge and hydraulic gradient where

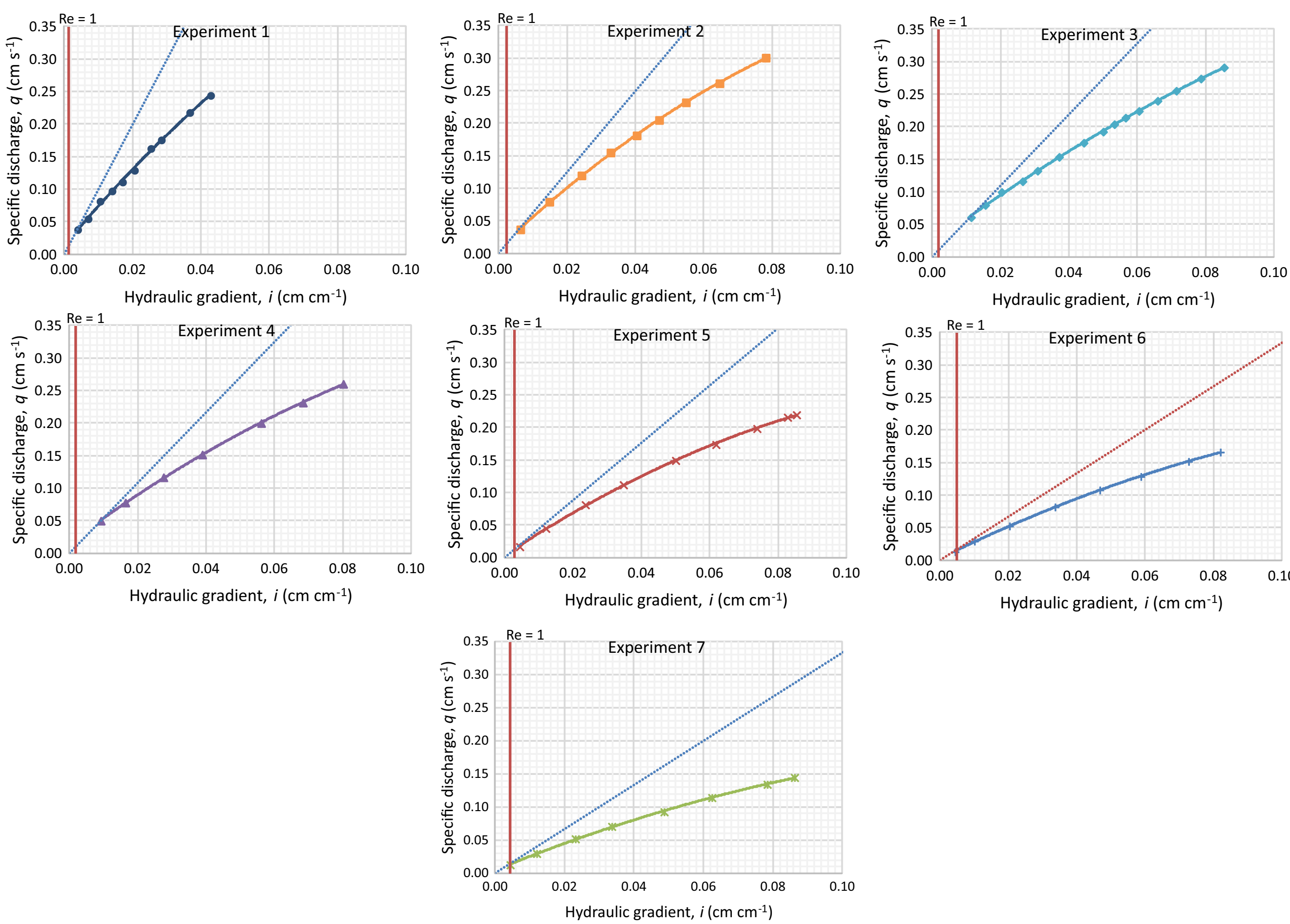

Fig. 3. Non-linear relationships between specific discharge and hydraulic gradient for old woodchips. The dotted lines pass through the point with the lowest hydraulic gradient to better illustrate the non-linearity. The red lines indicate the hydraulic gradient at which Reynolds number is equal to one.

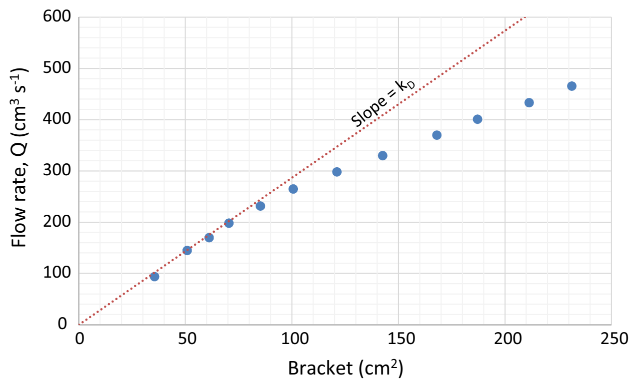

Fig. 4. Non-linear relationship between flow rate and the bracket component of Eq. (6) from a denitrification bed. Data from Ghane et al. (2014). Slope is equal to Darcy's hydraulic conductivity (k_D).

their specific discharge values were calculated across a range of temperatures from 6°C to 17°C. In their study, the presence of temperature as a confounding variable prevents establishing an outcome of specific discharge as being a direct consequence of hydraulic gradient. This is because temperature affects specific discharge (Section 4.9.1). Hence, the data presented in this section were obtained under minimal outflow temperature variations (20.1°C ± 0.6°C, average ± SD).

Based on laboratory column and field experiments, a linear relationship could not explain water flow through old woodchips. Thus, a non-Darcian equation is required to describe the flow pattern unless Darcian flow is validated for that situation. In other words, two parameters are needed to describe the curvilinear nature of the flow pattern (Section 2.1). In contrast, Darcy's equation (i.e., a one-parameter equation) can describe the linear flow pattern, but when used in modeling and design of beds with woodchip media, it can result in overestimation of the bed peak flow rate (Ghane et al., 2014). For example, if the bed design criterion is to treat a certain minimum flow rate (e.g., 15% of subsurface drainage peak flow), using Darcy's law could result in apparent satisfaction of that criterion while the criterion is actually not met.

4.3. Forchheimer's coefficients

We determined Forchheimer's coefficients based on the plot of hydraulic gradient versus specific discharge. Forchheimer's equation (Eq. (2)) was able to describe more than 99% (R-square) of the variation in all experiments (Supplementary File 1). The ω ranged from 0.22 to 1.61 indicating post-linear regime because ω was above zero (Table 1). The intrinsic permeability ranged from 2.9×10^{-5} to 8.0×10^{-5} cm^2 for the old woodchips, corresponding to hydraulic conductivities from 2.2 to 6.0 cm s^{-1} at 10°C, respectively.

Our intrinsic permeability of 2.9×10^{-5} cm^2 (and $\omega = 1.61$) at drainable porosity of 0.37 (experiment 7) was similar to that of 3.1×10^{-5} cm^2 (and $\omega = 2.02$) from the old woodchip laboratory experiment 1 of Ghane et al. (2014) that had the same drainable porosity. Although these two old woodchips had different sources (Minnesota and Ohio, USA), we found similarities in Forchheimer's coefficients between them under the same drainable porosity. Therefore, drainable porosity could be an important parameter for estimating Forchheimer's coefficients for woodchips when only the former is known. The empirical relationships between drainable porosity and Forchheimer's coefficients are discussed in Section 4.5.3.

Ghane et al. (2014) determined an in-situ intrinsic permeability and ω of 5.7×10^{-5} cm^2 and 0.88 for a bed in Ohio, respectively. Our intrinsic permeability and ω values from experiments 3 and 4 are similar to the in-situ values of 5.7×10^{-5} cm^2 and 0.88 reported by Ghane et al. (2014). Since these in-situ values are the only values reported so far, we assume that the bed in Ohio closely represents a denitrification bed under field conditions. This suggests that experiments 3 and 4 were close to field conditions in terms of pore structure. Therefore, we recommend using a woodchip compaction procedure that results in similar hydraulic properties to experiments 3 and 4 for investigating hydraulics and nitrate removal in laboratory column studies. This will result in laboratory experiments that represent the pore structure in the field more closely. Furthermore, similar values to our hydraulic properties of old woodchips (experiments 3 and 4) can be used in modeling studies and bed design (with similar particle size) when these values cannot be measured directly. This will allow a more accurate prediction of bed flow rate, and will result in a more efficient design.

4.3.1. Three dependent experiments

Results from the used batch of the composite old woodchips showed an increase in intrinsic permeability (Table 2). Intrinsic permeability from experiment U-2 was 35% greater than that of experiment 3 at the same drainable porosity of 0.41, and experiment U-3 was 47% greater than that of experiment 7 at the same drainable porosity of 0.37. We can attribute this increase of intrinsic permeability to flushing of fine woodchips and sediments. During the seven independent experiments, fine woodchips and sediments were observed in the water drained from the bottom of the column. However, there is a natural supply of sediments in drainage water feeding into a bed as well as woodchip particles breaking down during degradation. Ghane et al. (2014) also showed lower intrinsic permeability for old woodchips with sediments and fines than fresh woodchips without it. This shows that

Table 1
Summary of porosity, and the coefficients of Forchheimer and Izbash for old woodchips.

Experiment	Average outflow temperature ± SD (°C)	Drainable porosity, n_d	Forchheimer			Izbash		
			Intrinsic permeability, k_{in} (cm^2)	ω (s^2 cm^{-2})	Hydraulic conductivity at 10°C, k_F (cm s^{-1})	Permeability coefficient, M (cm s^{-1})	Permeability coefficient at 10°C, M_{10} (cm s^{-1})	Non-Darcy exponent, n
1	21.5 ± 0.1	0.43	8.0×10^{-5}	0.22	6.0	2.9	2.2	0.79
2	11.0 ± 0.2	0.43	8.0×10^{-5}	0.32	6.0	2.6	2.6	0.84
3	21.4 ± 0.2	0.41	5.6×10^{-5}	0.40	4.2	1.9	1.4	0.77
4	22.0 ± 0.0	0.41	5.6×10^{-5}	0.52	4.2	1.8	1.3	0.76
5	17.9 ± 0.3	0.40	4.6×10^{-5}	0.71	3.5	1.9	1.5	0.86
6	10.1 ± 0.0	0.38	4.1×10^{-5}	1.00	3.0	1.8	1.5	0.87
7	18.6 ± 0.2	0.37	2.9×10^{-5}	1.61	2.2	1.1	0.9	0.82

Table 2
Summary of porosity, and the coefficients of Forchheimer and Izbash from the dependent experiments that packed the used batch of old woodchips.

Dependent experiment	Average outflow temperature ± SD (°C)	Drainable porosity, n_d	Forchheimer			Izbash		
			Intrinsic permeability, k_{in} (cm^2)	ω (s^2 cm^{-2})	Hydraulic conductivity at 10°C, k_F (cm s^{-1})	Permeability coefficient, M (cm s^{-1})	Permeability coefficient at 10°C, M_{10} (cm s^{-1})	Non-Darcy exponent, n
U-1[a]	11.0 ± 0.1	0.45	1.5×10^{-4}	0.13	11.1	5.6	5.5	0.90
U-2[b]	10.5 ± 0.2	0.41	7.5×10^{-5}	0.35	5.6	3.1	3.0	0.91
U-3[b]	14.0 ± 0.1	0.37	4.3×10^{-5}	0.76	3.2	1.7	1.5	0.86

[a] Woodchips re-used once.
[b] Woodchips re-used twice.

sediments and fine woodchips play an important role in the hydraulic properties of old woodchips. Therefore, the permeability values for woodchips that have their sediments and fines flushed may not represent the flow under field conditions.

4.4. Izbash's coefficients

We determined Izbash's coefficients based on the plot of log specific discharge versus log hydraulic gradient (Fig. 5). The non-Darcy exponent (n) ranged from 0.76 to 0.87, which indicates post-linear regime since n was below one (Table 1). For Izbash's equation, as n reaches 0.5, flow becomes fully turbulent. The permeability coefficient (M_{10}) at 10°C ranged from 0.9 to 2.6 cm s^{-1} for the various drainable porosities. Although Forchheimer's hydraulic conductivity and Izbash's permeability coefficient have the same units (cm s^{-1}), they are different under post-linear flows (when $0.5 < n < 1$, then $k_F \neq M$). The reason for this difference (Table 1) is that Izbash's equation is empirical with a defined coefficient while that of Forchheimer's allows a theoretical calculation of hydraulic conductivity.

4.5. Drainable porosity

4.5.1. Laboratory experiments

Laboratory experiments resulted in drainable porosities (n_d) ranging from 0.37 to 0.43 for the three-year, eleven-month old woodchips (Table 1). Previous studies have calculated drainable porosities of 0.37 to 0.39 for the two-year, two-month old

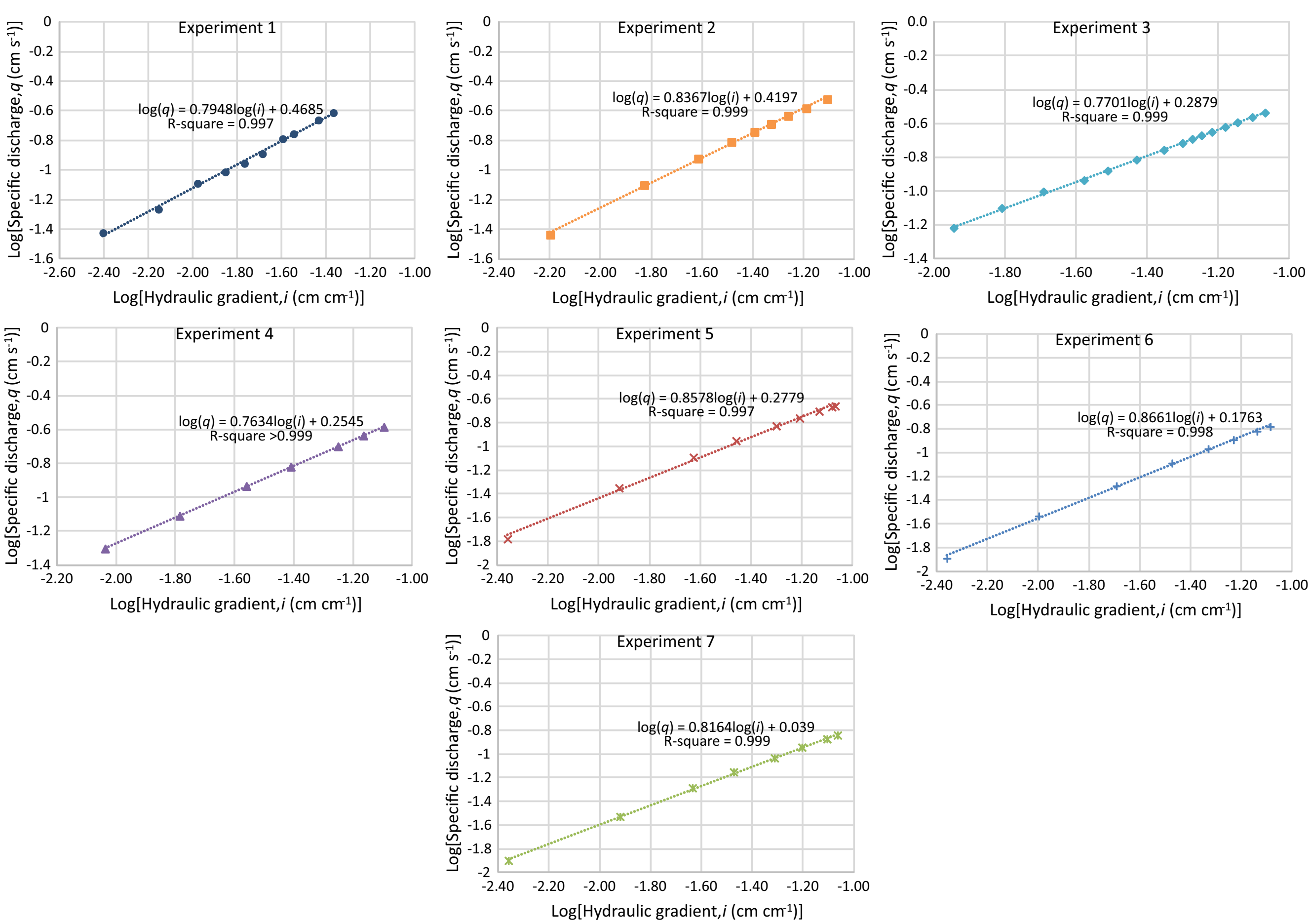

Fig. 5. Plots of log specific discharge versus log hydraulic gradient for determining Izbash's coefficients.

woodchips (Ghane et al., 2014), and 0.46 for seven-year old woodchips when draining the water for 1 h (Robertson, 2010). It has been shown that drainable porosity is smaller for old woodchips that have been under field conditions in a bed for a couple of years than fresh woodchips due to degradation and the presence of drainage-water sediments (Robertson, 2010; Ghane et al., 2014).

Some studies have assumed drainable porosities for beds under field conditions. Bell et al. (2015) assumed a drainable porosity of 0.70, and more recently, Rambags et al. (2016) assumed a drainable porosity of 0.70 for woodchips (10–30 mm size). To our knowledge, their assumed drainable porosity of 0.70 is the highest ever reported for any woodchips. Based on laboratory experiments of old woodchips (Robertson, 2010; Ghane et al., 2014), a drainable porosity closer to 0.40–0.45 is more realistic of woodchips under field conditions. The consequence of using an overly large drainable porosity is that it will result in overestimation of the actual hydraulic retention time.

4.5.2. Application of drainable porosity

One important application of drainable porosity is that it can be used instead of effective porosity to calculate the actual hydraulic retention time (*HRT*) when the latter is unavailable from tracer testing. This is because drainable porosity (specific yield) is almost equal to effective porosity (Sen, 2015). Effective porosity is the interconnected pores that are capable of transmitting water (Fetter, 2001; Sen, 2015), and it is used to calculate the actual hydraulic retention time (*HRT*) (Kadlec and Wallace, 2009). Some studies have calculated the actual *HRT* using drainable porosities ranging from 0.45 to 0.59 (Ghane et al., 2015; Feyereisen et al., 2016; Hoover et al., 2016), and some have used porosities ranging from 0.65 to 0.72 (Woli et al., 2010; Christianson et al., 2013; Lepine et al., 2016; Jaynes et al., 2016).

Porosity is defined as the ratio of volume of the void to the total volume of woodchips, which is equal to the summation of drainable porosity (specific yield) and specific retention (Bear, 1988; Fetter, 2001; Sen, 2015; Ward et al., 2016). Specific retention is the water volume retained against gravity, which describes the water content held inside woodchip particles. Since this water is held inside woodchip pores, its content has been determined from drying of gravity-drained woodchips using a fume hood and an oven (Robertson, 2010; Ghane et al., 2014). Thus, the entire water content held inside woodchip pores likely does not contribute to the active flow of water. In other words, a portion of the internal porosity may contribute to the active flow of water, but its quantity is currently unknown. Therefore, we advise caution in using overly large porosities (i.e., >0.65), since it may result in overestimation of the actual *HRT*. We recommend determining the effective porosity of beds under field conditions using tracer testing to ascertain the extent of the internal porosity involved in the active flow of water.

4.5.3. Relationship between drainable porosity and flow coefficients

Results from Izbash's equation (Eq. (3)) from Table 1 showed a significant power law relationship between drainable porosity and permeability coefficient at 10°C that explained 66.4% of the variation (Fig. 6). However, there was no significant power law relationship between drainable porosity and non-Darcy exponent (p-value = 0.374 and R-square = 0.160), and between the permeability coefficient at 10°C and non-Darcy exponent (p-value = 0.749 and R-square = 0.022).

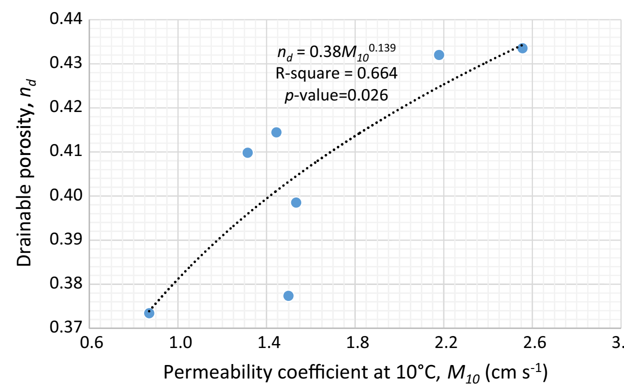

Fig. 6. Linear relationship between drainable porosity and Izbash's permeability coefficient at 10°C for old woodchips. R-square and p-value are for the linear relationships between the log of the two parameters.

Results from Forchheimer's equation (Eq. (2)) from Table 1 showed that drainable porosity and intrinsic permeability had a strong inverse relationship with ω (Fig. 7). Furthermore, we found a strong power law relationship between drainable porosity and intrinsic permeability for old woodchips. Ghane et al. (2014) also found a direct relationship between n_d and k_{in} when combining their laboratory data from both fresh and old woodchips. Therefore, our results show that drainable porosity and Forchheimer's coefficients can be estimated from one another based on our empirical relationships when one of them is known.

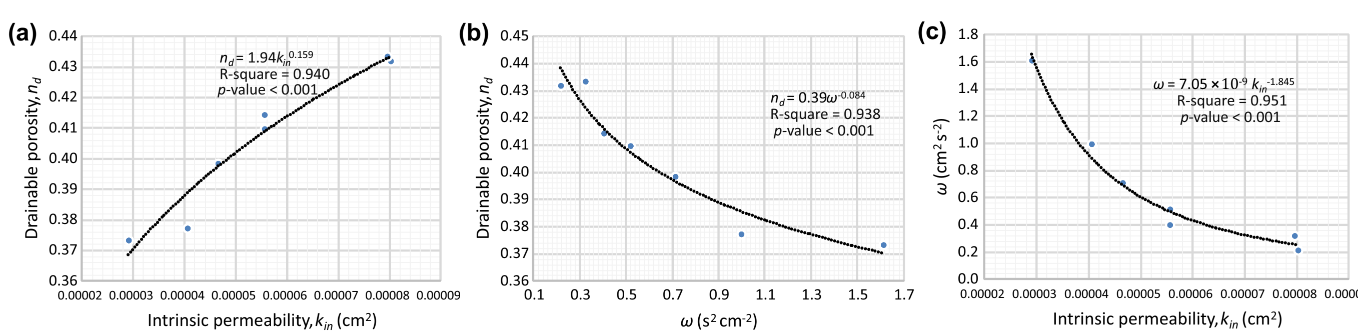

Fig. 7. Relationships between (a) n_d and k_{in}, (b) n_d and ω, and (c) ω and k_{in} for old woodchips. R-square and p-value are for the linear relationships between the log of the two parameters.

As woodchips get more compacted, their drainable porosity diminishes. Feyereisen and Christianson (2015) also found lower drainable porosity with greater compaction of fresh woodchips. Fig. 7a shows that as drainable porosity diminishes with more compaction, intrinsic permeability declines because there are smaller pore spaces available for flow. In terms of bed design, it may be better to cover beds with the minimum required soil depth (e.g., 15–30 cm), or to leave them without a soil cover if feasible, to minimize woodchip compaction. This will help avoid unnecessary flow capacity reduction in a bed. In terms of the potential of soil cover mitigating greenhouse gas emissions from the bed surface, there may not be a negative consequence of not covering beds with soil cover. This is because nitrous oxide emissions from the surface of beds (without soil cover) treating drainage water under field conditions have been negligible (Woli et al., 2010; Ghane et al., 2015; David et al., 2016).

Using the Run #2 flow data for fresh woodchips in Feyereisen and Christianson (2015), we calculated Izbash's ($M_{10} = 3.3$ cm s^{-1} and $n = 0.70$), and Forchheimer's ($k_{in} = 2.8 \times 10^{-4}$ cm^2 and $\omega = 0.01$ s^2 cm^{-2}) coefficients for a drainable porosity of 0.49 with a maximum hydraulic gradient of 0.087. The above-mentioned intrinsic permeability corresponds to Forchheimer's hydraulic conductivity of 20.8 cm s^{-1} at 10°C. The greater intrinsic permeability of the authors' Run #2 than that of experiment 1 of our study ($k_{in} = 8.0 \times 10^{-5}$ cm^2) is consistent with having a greater drainable porosity (0.49 versus 0.43). This is in accordance with our finding of direct relationship between n_d and k_{in}.

4.5.4. Estimation of in-situ drainable porosity

Ghane et al. (2014) used their power law relationship between n_d and k_{in} (i.e., determined from laboratory column experiments) to estimate an in-situ n_d of 0.45 based on their calculated in-situ k_{in} of 5.7×10^{-5} cm^2 for their bed. Using the same procedure, our empirical equation (Fig. 7a) resulted in an estimated in-situ n_d of 0.41 based on the in-situ k_{in} of 5.7×10^{-5} cm^2 from Ghane et al. (2014). These two estimated in-situ drainable porosity values (i.e., 0.41 and 0.45) are close to the range of n_d determined in our laboratory experiments for old woodchips (Table 1). Since Ghane et al. (2014) used a bed that was more than two years old, we believe that their in-situ k_{in} calculation, and in turn, our n_d estimate represents a bed operating past its initial stages. This is because woodchips in a bed subside and undergo carbon loss in the early stages of operation, but become relatively stable after this period (Robertson, 2010). The results of this section agree with the finding that drainable porosity closer to 0.40–0.45 is more realistic of woodchips under field conditions than those studies with much greater values.

4.6. Comparing Forchheimer with Izbash

When comparing Forchheimer's to Izbash's equation, the former provided a better fit to the data, which was reflected in its superior average R-square (i.e., 0.9997 ± 0.0006 vs. 0.9985 ± 0.0013) (Supplementary File 1 and Fig. 5). Furthermore, the coefficients of the former (k_{in} and ω) provided stronger empirical relationships with drainable porosity (Section 4.5.3). The practical importance of strong relationships is that when one of the values is known, the other can be estimated. Izbash's equation is empirical and does not provide an accustomed hydraulic conductivity value for soil scientists and engineers. Instead, it provides a permeability coefficient, which is different from hydraulic conductivity. On the other hand, Forchheimer's equation has a theoretical basis (Irmay, 1958) and provides an accustomed hydraulic conductivity value. Therefore, we recommend Forchheimer's equation over that of Izbash's for describing water flow through woodchips.

4.7. Reynolds number

We used the lowest hydraulic gradient as the critical point beyond which flow enters post-linear regime, since the next higher hydraulic gradient did not form a linear line with that of the lowest (Fig. 3). Thus, we used the critical point to determine the critical Reynolds number, Forchheimer number and the non-Darcy effect (Table 3). Water flow through porous media is usually referred to as laminar when Reynolds number is below 1.0 (Fetter, 2001; Bear, 1988). Our experiments showed critical Reynolds numbers ranging from 0.9 to 5.7 corresponding to hydraulic gradients of 0.004 to 0.011, respectively, which means that Reynolds number exceeded one at higher hydraulic gradients. Our critical Reynolds numbers for old woodchips are similar to that of 2.3 to 3.1 from Ghane et al. (2014).

Table 3
Critical values beyond which flow enters post-linear regime based on graphical evaluation of non-Darcy flow of old woodchips.

Experiment	Critical hydraulic gradient (cm cm^{-1})	Critical Reynolds number	Critical Forchheimer number	Critical non-Darcy effect
1	0.004	3.5	0.07	0.06
2	0.006	2.6	0.07	0.07
3	0.011	5.7	0.14	0.12
4	0.009	4.7	0.15	0.13
5	0.004	1.4	0.05	0.05
6	0.004	0.9	0.04	0.04
7	0.004	1.1	0.06	0.05

4.8. Forchheimer number and non-Darcy effect

The critical Forchheimer number and non-Darcy effect for old woodchips averaged 0.08 ± 0.04 and 0.07 ± 0.04 (Table 3). This means that the error of ignoring the non-Darcy flow in old woodchips was on average at least 7% at the average hydraulic gradient of 0.006 ± 0.003. It is important to note that this error will increase during bed peak flows due to rise in hydraulic gradient. Zeng and Grigg (2006) suggest a 10% limit for the non-Darcy effect as a good reference. Macini et al. (2011) found a higher average non-Darcy effect of 28% for natural sand.

Ghane et al. (2014) reported a critical non-Darcy effect of 0.16 for their old woodchip experiment 1 compared to that of 0.05 from our experiment 7 with a similar drainable porosity of 0.37. This difference in non-Darcy effect could be the result of the difference in the two permeameters. Our permeameter allowed measurements to initiate from a lower hydraulic gradient (i.e., 0.004 in experiment 7) than that from Ghane et al. (2014) (i.e., 0.018 for their experiment 1). This allowed us to detect non-linearity at a lower critical hydraulic gradient, whereas the other study had to assume the critical hydraulic gradient initiated at their lowest hydraulic gradient because they did not have a lower hydraulic gradient to assess non-linearity (Supplementary File 2). Overall, we emphasize the need to account for non-Darcy flow of water through old woodchips at high water velocities.

4.9. Temperature effects on hydraulic properties

4.9.1. Temperature effects on hydraulic conductivity

In our study, experiments 1 and 2 resulted in similar hydraulic properties (k_{in}, ω and n_d) while conducted at average outflow temperatures of 21.5°C and 11.0°C, respectively (Table 1). The plot of these two experiments shows the effect of temperature on

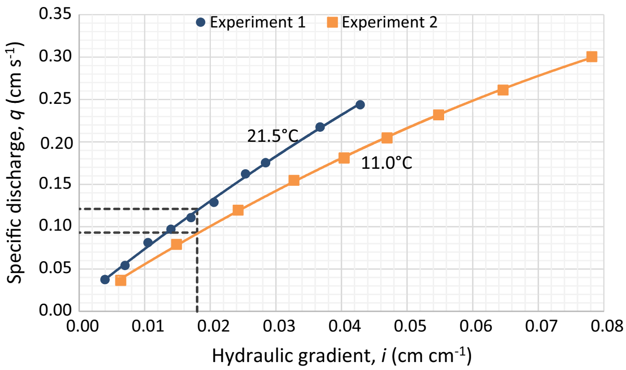

Fig. 8. Graph showing the effect of temperature on specific discharge for two experiments with similar hydraulic properties. The dotted lines show a q of 0.121 and 0.093 cm s^{-1} for experiments 1 and 2 at $i = 0.018$, respectively.

specific discharge (Fig. 8). At any hydraulic gradient, the warmer water shows 1.3 times (i.e., also equal to $\mu_{11.0}/\mu_{21.5} = 0.01271/0.00968$) larger specific discharge than that of the colder water. Furthermore, the larger specific discharge of the warmer water translates into a larger flow rate. Hence, in our experiments, we allowed the outflow temperature to stabilize before taking measurements to eliminate the confounding effect of temperature on specific discharge (Section 3.3.3). Therefore, accounting for temperature effects on water flow through denitrification beds is vital to the design and modeling of these systems.

4.9.2. Temperature effects on drainable porosity

In our study, we drained the columns immediately after each experiment, and vast majority of the water volume was drained within the first hour. Thus, the average outflow temperatures in Table 1 represent the temperature at which water was drained. We did not observe any influence of temperature on drainable porosity based on experiments 1 and 2. These two experiments resulted in a drainable porosity of 0.43 while the former was at 21.5°C and the latter was at 11.0°C.

Our observation is consistent with the fresh woodchip experiments 2 and 4 (with identical $k_{in} = 1.4 \times 10^{-4}$ cm^2) from Ghane et al. (2014) where they reported a drainable porosity of 0.56 at 12°C and 8°C, respectively. In contrast, Cameron and Schipper (2012) concluded that drainable porosity was significantly greater for their 23.5°C woodchip columns than that with the 14.0°C at the end of their trial. However, we could not find the drainable porosities of the columns under the same temperature at the end of their trial to verify if the columns being compared had identical drainable porosities. Woodchip columns should have identical drainable porosities at the same temperature before determining the effect of temperature on drainable porosity. Therefore, our results show no evidence of temperature affecting drainable porosity.

5. Conclusions

We graphically confirmed non-Darcy flow through old woodchips based on column experiments, and for the first time, in a denitrification bed under field conditions. Based on the Forchheimer number, the error of ignoring the non-Darcy flow in old woodchips was on average at least 7% at the average hydraulic gradient of 0.006 ± 0.003 with a greater error occurring at higher hydraulic gradients (i.e., at bed peak flows). Results showed that similar values to the hydraulic properties of old woodchips in experiment 3 and 4 can be used in modeling studies and bed design (with similar particle size) when these values are unavailable. Furthermore, experiments with the used batch of the old woodchips resulted in up to 47% greater intrinsic permeability. This shows that sediments and fine woodchips play an important role in the flow of water through woodchips, so this should be considered when determining the hydraulic properties of woodchips.

The direct relationship between intrinsic permeability and drainable porosity indicated that woodchip compaction plays an important role in reducing flow capacity of denitrification beds. We estimated an in-situ drainable porosity of 0.41 for a denitrification bed under field conditions that was close to a previous estimation of 0.45. We found that drainable porosity closer to 0.40–0.45 is more realistic of woodchips under field conditions than those with much greater values.

Comparison between Forchheimer's and Izbash's equations revealed that Forchheimer's equation was more suitable for water flow through woodchip media. Due to the non-Darcy flow characteristics, two coefficients (e.g., k_{in} and ω, or M and n) are needed to describe water flow through woodchips. Laboratory experiments showed no temperature influence on drainable porosity. Furthermore, we demonstrated the effect of temperature on specific discharge, so this effect should be considered when characterizing the hydraulic properties of woodchips.

In conclusion, this work characterizes the hydraulic properties of woodchips using non-Darcy equations, and provides a better understanding of the parameters affecting flow. These findings are important because they are required for designing denitrification beds with optimum nitrate removal and minimal undesirable consequences. We recommend that future research be focused on using non-Darcy flow characteristics of woodchips to adjust the current NRCS design guidelines for denitrification beds to yield more efficient systems.

Disclaimer

Mention of trade names or commercial products in this publication is solely for the purpose of providing specific information and does not imply recommendation or endorsement by the U.S. Department of Agriculture. USDA is an equal opportunity provider and employer.

Role of funding source

Funding of this research was provided in part by Minnesota Discovery, Research and Innovation Economy; Minnesota Soybean Research and Promotion Council; Minnesota Corn Research and Promotion Council; Minnesota Agricultural Water Resource Center, and Minnesota Turkey Research and Promotion Council. The funding sources were not involved in the study design, collection, analysis, interpretation of data, or preparation of the manuscript.

Acknowledgments

We express gratitude to Jacob Mattson and Brendan McShane for their assistance.

Appendix A. Supplementary material

Supplementary data associated with this article can be found, in the online version, at http://dx.doi.org/10.1016/j.jhydrol.2016.09.021. These data include Google map, videos, files, images, and interactive plots.

References

Basak, P., 1977a. Non-penetrating well in a semi-infinite medium with non-linear flow. J. Hydrol. 33, 375–382.
Basak, P., 1977b. Non-Darcy flow and its implications to seepage problems. J. Irrigation Drainage Div. ASCE 103, 459–473.

Bear, J., 1988. Dynamics of Fluids in Porous Media. American Elsevier Publishing Company Inc., NY, USA.
Bednarek, A., Szklarek, S., Zalewski, M., 2014. Nitrogen pollution from areas of intensive farming–comparison of various denitrification biotechnologies. Ecohydrol. Hydrobiol. 14, 132–141.
Bell, N., Cooke, R.A., Olsen, T., David, M.B., Hudson, R., 2015. Characterizing the performance of denitrifying bioreactors during simulated subsurface drainage events. J. Environ. Qual. 44, 1647–1656.
Bordier, C., Zimmer, D., 2000. Drainage equations and non-Darcian modelling in coarse porous media or geosynthetic materials. J. Hydrol. 228, 174–187.
Cameron, S.G., Schipper, L.A., 2010. Nitrate removal and hydraulic performance of organic carbon for use in denitrification beds. Ecol. Eng. 36, 1588–1595.
Cameron, S.G., Schipper, L.A., 2012. Hydraulic properties, hydraulic efficiency and nitrate removal of organic media for use in denitrification beds. Ecol. Eng. 41, 1–7.
Chen, Y., Zhou, J., Hu, S., Hu, R., Zhou, C., 2015. Evaluation of Forchheimer equation coefficients for non-Darcy flow in deformable rough-walled fractures. J. Hydrol. 529, 993–1006.
Christianson, L.E., Helmers, M.J., Bhandari, A., Moorman, T.B., 2013. Internal hydraulics of an agricultural drainage denitrification bioreactor. Ecol. Eng. 52, 298–307.
Chun, J.A., Cooke, R.A., Eheart, J.W., Kang, M.S., 2009. Estimation of flow and transport parameters for woodchip-based bioreactors: I. laboratory-scale bioreactor. Biosyst. Eng. 104, 384–395.
Dan, H.C., He, L.H., Xu, B., 2016. Experimental investigation on non-Darcian flow in unbound graded aggregate material of highway pavement. Transp. Porous Med. 112, 189–206.
Darcy, H., 1856. The Public Fountains of the City of Dijon. English translated by P. Bobeck, 2004. Kendall/Hunt Publishers, Dubuque, IA, USA.
David, M.B., Gentry, L.E., Cooke, R.A., Herbstritt, S.M., 2016. Temperature and substrate control woodchip bioreactor performance in reducing tile nitrate loads in east-central Illinois. J. Environ. Qual. 45, 822–829.
Fetter, C.W., 2001. Applied Hydrogeology. Prentice Hall Inc., Upper Saddle River, NJ, USA.
Feyereisen, G.W., Christianson, L.E., 2015. Hydraulic flow characteristics of agricultural residues for denitrifying bioreactor media. Appl. Eng. Agric. 31, 89–96.
Feyereisen, G.W., Moorman, T.B., Christianson, L.E., Venterea, R.T., Coulter, J.A., Tschirner, U.W., 2016. Performance of agricultural residue media in laboratory denitrifying bioreactors at low temperatures. J. Environ. Qual. 45, 779–787.
Forchheimer, P.H., 1901. Wasserbewegung durch Boden. ZVDI 45, 1781–1788.
Gao, H., Shao, M., 2015. Effects of temperature changes on soil hydraulic properties. Soil Till. Res. 153, 145–154.
Ghane, E., Fausey, N.R., Brown, L.C., 2014. Non-Darcy flow of water through woodchip media. J. Hydrol. 519, 3400–3409.
Ghane, E., Fausey, N.R., Brown, L.C., 2015. Modeling nitrate removal in a denitrification bed. Water Res. 71, 294–305.
Goodwin, G.E., Bhattarai, R., Cooke, R.A., 2015. Synergism in nitrate and orthophosphate removal in subsurface bioreactors. Ecol. Eng. 84, 559–568.
Harke, M.J., Gobler, C.J., 2015. Daily transcriptome changes reveal the role of nitrogen in controlling microcystin synthesis and nutrient transport in the toxic cyanobacterium, *Microcystis aeruginosa*. BNC Genom. 16, 1068.
Hoover, N.L., Bhandari, A., Soupir, M.L., Moorman, T.B., 2016. Woodchip denitrification bioreactors: Impacts of temperature and hydraulic retention time on nitrate removal. J. Environ. 45, 803–812.
Hopes, G.M., 2010. Hydraulic Evaluation of Wood Chip Media Constructed Wetlands for Denitrification M.S. Thesis. University of California, Davis, CA, USA.
Horst, G.P., Sarnelle, O., White, J.D., Hamilton, S.K., Kaul, R.B., Bressie, J.D., 2014. Nitrogen availability increases the toxin quota of a harmful cyanobacterium, *Microcystis aeruginosa*. Water Res. 54, 188–198.
Hubert, M.K., 1940. The theory of ground-water motion. J. Hydrol. 48, 785–944.
Irmay, S., 1958. On the theoretical deviation of Darcy and Forchheimer formulas. EOS T. Am. Geophys. Un. 39, 702–707.
Izbash, S.V., 1931. O Filtracii V Kropnozernstom Materiale. Izv. Nauchnoissled, Inst. Gidrotechniki, Leningrad, USSR.
Jaynes, D.B., Moorman, T.B., Parking, T.B., Kaspar, T.C., 2016. Simulating woodchip bioreactor performance using a dual-porosity model. J. Environ. Qual. 45, 830–838.
Kadlec, R.H., Wallace, S.D., 2009. Treatment Wetlands. CRC Press, Boca Raton, FL, USA.
Krause Camilo, B., 2016. Bioreactor reduces atrazine and nitrate in tile drain waters. Ecol. Eng. 86, 269–278.
Krause Camilo, B., Matzinger, A., Litz, N., Tedesco, L.P., Wessolek, G., 2013. Concurrent nitrate and atrazine retention in bioreactors of straw and bark mulch at short hydraulic residence times. Ecol. Eng. 55, 101–113.
Lepine, C., Christianson, L.E., Sharrer, K., Summerfelt, S., 2016. Optimizing hydraulic retention times in denitrifying woodchip bioreactors treating recirculating aquaculture system wastewater. J. Environ. Qual. 45, 813–821.
Leverenz, H.L., Haunschild, K., Hopes, G.M., Tchobanoglous, G., Darby, J.L., 2010. Anoxic treatment wetlands for denitrification. Ecol. Eng. 36, 1544–1551.
Macini, P., Mesini, E., Viola, R., 2011. Laboratory measurements of non-Darcy flow coefficients in natural and artificial unconsolidated porous media. J. Petrol. Sci. Eng. 77, 365–374.
Rambags, F., Tanner, C.C., Stott, R., Schipper, L.A., 2016. Fecal bacteria, bacteriophage, and nutrient reductions in a full-scale denitrifying woodchip bioreactor. J. Environ. Qual. 45, 847–854.
Robertson, W.D., 2010. Nitrate removal rates in woodchip media of varying age. Ecol. Eng. 36, 1581–1587.
Robertson, W.D., Ptacek, C.J., Brown, S.J., 2009. Rates of nitrate and perchlorate removal in a 5-year-old wood particle reactor treating agricultural drainage. Ground Water Monit. R. 29, 87–94.
Robertson, W.D., Merkley, L.C., 2009. In-stream bioreactor for agricultural nitrate treatment. J. Environ. Qual. 38, 230–237.
Sadeghi-Asl, M., Rahimi, H., Salehi, R., 2014. Non-Darcy flow of water through a packed column test. Transp. Porous Med. 101, 215–227.
Schipper, L.A., Robertson, W.D., Gold, A.J., Jaynes, D.B., Cameron, S.G., 2010. Denitrifying bioreactors-an approach for reducing nitrate loads to receiving water. Ecol. Eng. 36, 1532–1543.
Schmidt, C.A., Clark, M.W., 2013. Deciphering and modeling the physicochemical drivers of denitrification rates in bioreactors. Ecol. Eng. 60, 276–288.
Sen, Z., 2015. Practical and Applied Hydrogeology. Elsevier Inc., Amsterdam, The Netherlands.
Shih, R., Robertson, W.D., Schiff, S.L., Rudolph, D.L., 2011. Nitrate controls methyl mercury production in a streambed bioreactor. J. Environ. Qual. 40, 1586–1592.
Soni, J.P., Islam, N., Basak, P., 1978. An experimental evaluation of non-Darcian flow in porous media. J. Hydrol. 38, 231–241.
Subroy, V., Gimenez, D., Qin, M., Krogmann, U., Strom, P.F., Miskewitz, R.J., 2014. Hydraulic properties of coarsely and finely ground woodchips. J. Hydrol. 517, 201–212.
USDA NRCS, 2015. Conservation Practice Standard: Denitrifying Bioreactor. Code 605. United States Department of Agriculture, Natural Resources Conservation Service, Washington, DC, USA.
USEPA, 2013. Reassessment 2013: Assessing Progress Made Since 2008. Mississippi River Gulf of Mexico Watershed Nutrient Task Force. United States Environmental Protection Agency, Washington, DC, USA.
Van Driel, P.W., Robertson, W.D., Merkley, L.C., 2006. Denitrification of agricultural drainage using wood-based reactors. Trans. Am. Soc. Agric. Biol. Eng. 49, 565–573.
Wang, Q., Zhan, H., Wang, Y., 2015. Non-Darcian effect on slug test in a leaky confined aquifer. J. Hydrol. 527, 747–753.
Ward, A.D., Trimble, S.W., Burckhard, S.R., Lyon, J.G., 2016. Environmental Hydrology. CRC Press, Boca Raton, FL, USA.
Wen, Z., Liu, K., Chen, X., 2013. Approximate analytical solution for non-Darcian flow toward a partially penetrating well in a confined aquifer. J. Hydrol. 498, 124–131.
Woli, K.P., David, M.B., Cooke, R.A., McIsaac, G.F., Mitchell, C.A., 2010. Nitrogen balance in and export from agricultural fields associated with controlled drainage systems and denitrifying bioreactors. Ecol. Eng. 36, 1558–1566.
Zeng, Z., Grigg, R., 2006. A criterion for non-Darcy flow in porous media. Transp. Porous Med. 63, 57–69.